Journal of Nuclear Materials 386–388 (2009) 60–63

Contents lists available at ScienceDirect

Journal of Nuclear Materials

journal homepage: www.elsevier.com/locate/jnucmat

Magnetic properties of point defect interaction with impurity atoms in Fe–Cr alloys

D. Nguyen-Manh *, M.Yu. Lavrentiev, S.L. Dudarev

EURATOM/UKAEA Fusion Association, Culham Science Centre, Oxfordshire OX14 3DB, UK

ARTICLE INFO

PACS:
61.72.Ji
61.82.Bg
71.15.Mb
71.10.Be
75.10.Lp

ABSTRACT

An integrated *ab initio* and statistical Monte Carlo investigation has been recently carried out to model the thermodynamic and kinetic properties of Fe–Cr alloys. We found that the conventional Fe–Cr phase diagram is not adequate at low temperature region where the magnetic contribution to the free energy plays an important role in the prediction of an ordered $Fe_{15}Cr$ phase and its negative enthalpy of formation. The origin of the anomalous thermodynamic and magnetic properties of Fe–Cr alloys can be understood using a tight-binding Stoner model combined with the charge neutrality condition. We investigate the environmental dependence of magnetic moment distributions for various self-interstitial atom ⟨1 1 0⟩ dumbbells configurations using spin density maps found using density functional theory calculations. The mixed dumbbell Fe–Cr and Fe–Mn binding energies are found to be positive due to magnetic interactions. Finally, we discuss the relationship between the migration energy of vacancy in Fe–Cr alloys and magnetism at the saddle point configuration.

1. Introduction

Body-centred cubic Fe–Cr alloys form the basis of many industrially important steels. Following the discovery of their high swelling resistance in tests performed in fission reactors during the 1990s, the low-activated ferritic/martensitic steels (LAMS) with 7–12 wt% Cr have been selected as candidate materials for structural applications in future power fusion plants for the range of operational temperatures below 550 °C [1]. However, these steels exhibit radiation hardening at low temperature and moderate irradiation doses. Therefore, it is important to understand the factors driving the evolution of microstructure that are linked to the degradation of mechanical properties in these alloys. In the absence of a dedicated intense neutron source of the 14 MeV neutrons from the D–T fusion reaction, the development of computational techniques capable of predicting changes in mechanical properties, microstructure, and phase stability of LAMS and Fe–Cr model alloys occurring under fusion-relevant irradiation conditions, is an important objective of fusion materials research.

Recently, a multi-scale modelling approach has been applied to the investigation of thermodynamic and kinetic properties of binary Fe–Cr alloys by combining density functional theory (DFT) calculations with statistical techniques involving cluster expansion and Monte Carlo simulations [2,3]. This makes it possible to generate, in a more systematic and accurate way, the lowest energy configurations from which point defects (vacancies and self-interstitial atoms (SIAs)) and their interactions at arbitrary Cr concentration can be investigated. At variance with previous theoretical and modelling studies of Fe–Cr alloys [4–6], where negative enthalpy of mixing was found for random or quasi-random configurations with short-range order interactions, our studies showed that this anomalous behaviour occurred for an ordered $Fe_{15}Cr$ phase, the stability of which was directly correlated with the presence of magnetic interactions in dilute Fe–Cr alloys. Within this picture, the phase diagram of a binary Fe–Cr alloy for concentrations exceeding 10% Cr can be interpreted as phase separation between the possibly partially disordered $Fe_{15}Cr$ α-phase and the α′ phase of bcc-Cr. Furthermore, clustering of Cr atoms is strongly correlated with magnetic properties of concentrated Cr alloys [7]. In this paper, we focus on the environmental dependence of magnetic properties of SIA and vacancy defect configurations in the ordered $Fe_{15}Cr$ phase and at low Cr concentrations. We investigate electron spin density maps produced using self-consistent DFT calculation within generalized gradient approximation (GGA).

2. The magnetic origin of thermodynamic properties of Fe–Cr alloys

The enthalpy of mixing of the Fe–Cr system has been recently re-investigated by combining spin-polarized DFT-GGA calculations performed within the VASP code [8,9] and the cluster expansion based exchange Monte Carlo simulations [2,3,7]. One of the significant results derived from these studies is that both DFT and Monte

* Corresponding author.
E-mail address: duc.nguyen@ukaea.org.uk (D. Nguyen-Manh).

0022-3115/$ - see front matter © 2009 Elsevier B.V. All rights reserved.
doi:10.1016/j.jnucmat.2008.12.059

Carlo models predict a long-range ordered structure at 6.25% Cr with negative (−6.5 meV/atom and −4.8 meV/atom, respectively) enthalpy of formation. Furthermore, within the homogenous Bragg–Williams approximation, where many-atom cluster interactions are neglected, we find that the mixing enthalpy exhibits behaviour similar to that found in EMTO-CPA calculations [5], showing that previous studies in fact addressed the high temperature limit of random alloy configuration of the Fe–Cr system.

The origin of the anomalous enthalpy of mixing at low Cr concentration can be explained using the tight-binding Stoner model (TBSM) developed from the previous studies of bcc-Fe [10,11,7]. Here the TBSM calculations were performed using the rigid-band approximation with the same TB parameterisation of 3d orbitals for both Fe and Cr as those found in Ref. [10]. The charge neutrality condition has been applied assuming the total electron occupancies of 6.8 for Fe and 5.5 for Cr, and the Stoner interaction parameter for the on-site magnetic interactions of 0.77 eV and 0.38 eV for Fe and Cr, respectively. The values of these parameters are consistent with those obtained from DFT calculations for the 3d magnetic transition metals in Ref. [12]. Fig. 1 shows comparison between DFT and TBSM results for the enthalpy of mixing for various Cr concentrations in different binaries: $Fe_{15}Cr$, $Fe_{25}Cr_2$, $Fe_{14}Cr_2$, $Fe_{18}Cr_{12}$, Fe_3Cr (DO3), FeCr (B2), $FeCr_3$ (DO3) and $FeCr_{15}$. Apart from the $Fe_{18}Cr_{12}$ alloy representing the σ-phase, other binaries are the bcc-like alloys. The $Fe_{25}Cr_2$ structure is taken from previous DFT studies [3,13]. We find excellent agreement between TBSM and DFT calculations on the cross-over from negative to positive values of the enthalpy of formation for all the cases considered in this study. In particular, for the ordered $Fe_{15}Cr$ phase, the formation energy obtained from TBSM calculation is −6.9 meV/atom. Fig. 2 shows the magnetic moment distributions (from $-1.7\mu_B$ to $2.3\mu_B$) calculated by both DFT and TBSM for the $Fe_{15}Cr$ structure. We see that the anti-ferromagnetic alignment of Cr atoms with respect to ferromagnetic Fe atoms is very well reproduced, confirming the occurrence of long-range order in $Fe_{15}Cr$ within *k*-space calculations in TBSM.

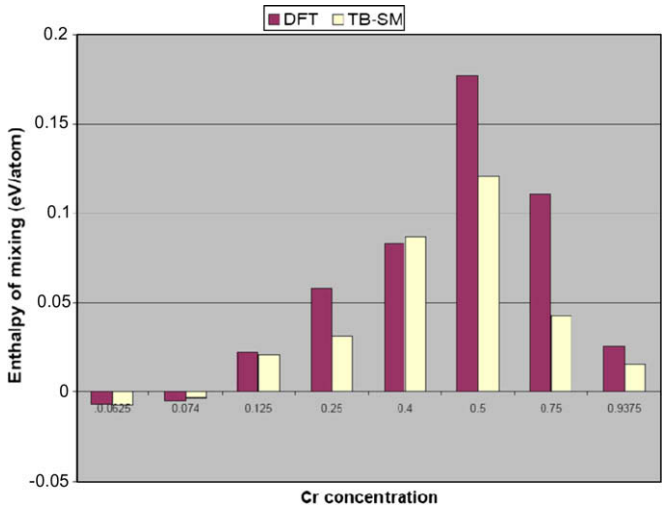

Fig. 1. Enthalpies of mixing calculated using the tight-binding Stoner model and compared with the corresponding DFT values for different Cr concentrations in Fe–Cr binary alloys.

3. Magnetic behaviour of SIA defects in ordered $Fe_{15}Cr$ phase

Recently, it has been suggested on the basis of electrical resistivity recovery measurements that specific features of electron-irradiated Fe–Cr concentrated alloys over the stage I temperature interval can be explained by the formation, migration and trapping of mixed dumbbells [14]. We have calculated formation and binding energies of the ⟨1 1 0⟩ Fe–Fe, Cr–Cr and Fe–Cr at the five different crystallographic sites associated with the space group symmetry of the ordered phase $Fe_{15}Cr$ and found that the most stable mixed dumbbell is located at the Fe_3 site where there are no Cr atoms in its environment up to the fifth nearest neighbours [2,15]. The formation and binding energies of this Fe–Cr mixed ⟨1 1 0⟩ dumbbell are 3.58 eV and 0.15 eV, respectively. Fig. 3 shows the spin density maps calculated within the DFT-GGA approach and projected on the (1 1 0) plane for different mixed Fe–Cr dumbbell (a) and Fe–Fe, Cr–Cr dumbbell (b) ⟨1 1 0⟩ configurations at four crystallographic positions (Fe_3, Fe1, Fe and Cr). It is clearly seen from Fig. 3(a) that the spin density map of the mixed dumbbell located at site Fe_3 (bottom right) can be distinguished from other ones by relatively high magnetic moment at Cr atom ($-0.9\mu_B$) whereas the magnetic moment at Fe is reduced to $0.7\mu_B$ at the SIA defect configuration in comparison with the average moment ($2.3\mu_B$) at Fe sites in the host matrix. We therefore find that there is correlation between the positive binding energy and Fe–Cr magnetic interaction at the mixed dumbbell defect. It is worth emphasizing that the point defect behaviour in the non-magnetic bcc transition metals is fundamentally different to that found in

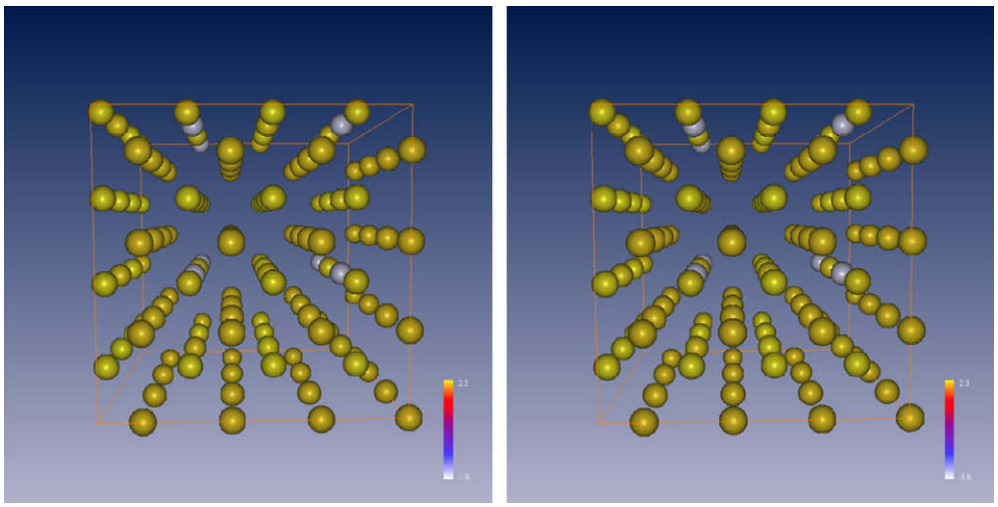

Fig. 2. Magnetic moment distribution in ordered phase $Fe_{15}Cr$ calculated within the tight-binding Stoner model (right) and compared with those obtained from DFT calculations (left). Grey atoms are the Cr ones with negative magnetic moments.

ferromagnetic bcc iron [16–18]. Among the different Fe–Fe and Cr–Cr ⟨1 1 0⟩ dumbbell configurations considered in Fig. 3(b), it is found that that magnetic moment for two Cr atoms at the SIA defect is also negative ($-0.5\mu_B$). However the formation energy of this Cr–Cr dumbbell (4.09 eV) is higher that those found at different Fe sites (3.71–3.75 eV). This is also consistent with the trend between Fe–Fe and Cr–Cr dumbbells in pure elements [16,17].

4. SIA-impurity interaction in $Fe_{15}Cr$ phase

Modelling of irradiation-induced segregation or thermal non-equilibrium segregation requires data on impurity-defect interaction energies. For ferritic/martensitic steels, the matter is more complex due to the presence of magnetic interaction that we discussed in the previous session for the binary Fe–Cr alloys. The previous approach for calculating impurity-interstitial (mixed dumbbell) binding energies on the basis of classical strain field arguments due to different over/undersize effects cannot be valid [19]. For example, following these arguments one could predict a negative binding energy (−0.096 eV) of mixed Fe–Cr dumbbell in ferritic steel matrix whereas our DFT calculations predict a positive binding energy. A systematic study of mixed dumbbell binding energies with non-magnetic transition metals elements (V, Nb, Mo, Ta, W) as well as with sp-valent element (P, S, Si, Al) was carried out in a previous study [15]. Fig. 4 shows the spin density maps calculated for mixed dumbbell configuration with manganese and carbon impurity atoms and also Mn–Mn dumbbell and octahedral C impurity at Fe_3 site in $Fe_{15}Cr$ phase. We find the mixed dumbbell Fe–Mn binding energy calculated is strongly positive (0.34 eV) that is again correlated with the anti-ferromagnetic spin of $-0.7\mu_B$ shown in the top left of Fig. 4. Taking into account that the Mn atom is an oversized impurity in comparison with Fe (1.36 Å vs. 1.24 Å) the present result together with those shown Fig. 3(a) for the Fe–Cr mixed dumbbell demonstrate a crucial role played by magnetic contribution to the binding energy of SIA-impurity interaction. The spin density maps for carbon impurity show a very small magnetic moment ($-0.08\mu_B$) for both interstitial and octahedral site and in these cases the positive binding energies found from DFT calculations can be understood from the strain field theory arguments. The latter case (with carbon impurity) gives a consistent result with our previous study on mixed dumbbells between Fe and P, S, Si and Al [15] where the size effect plays a dominant role.

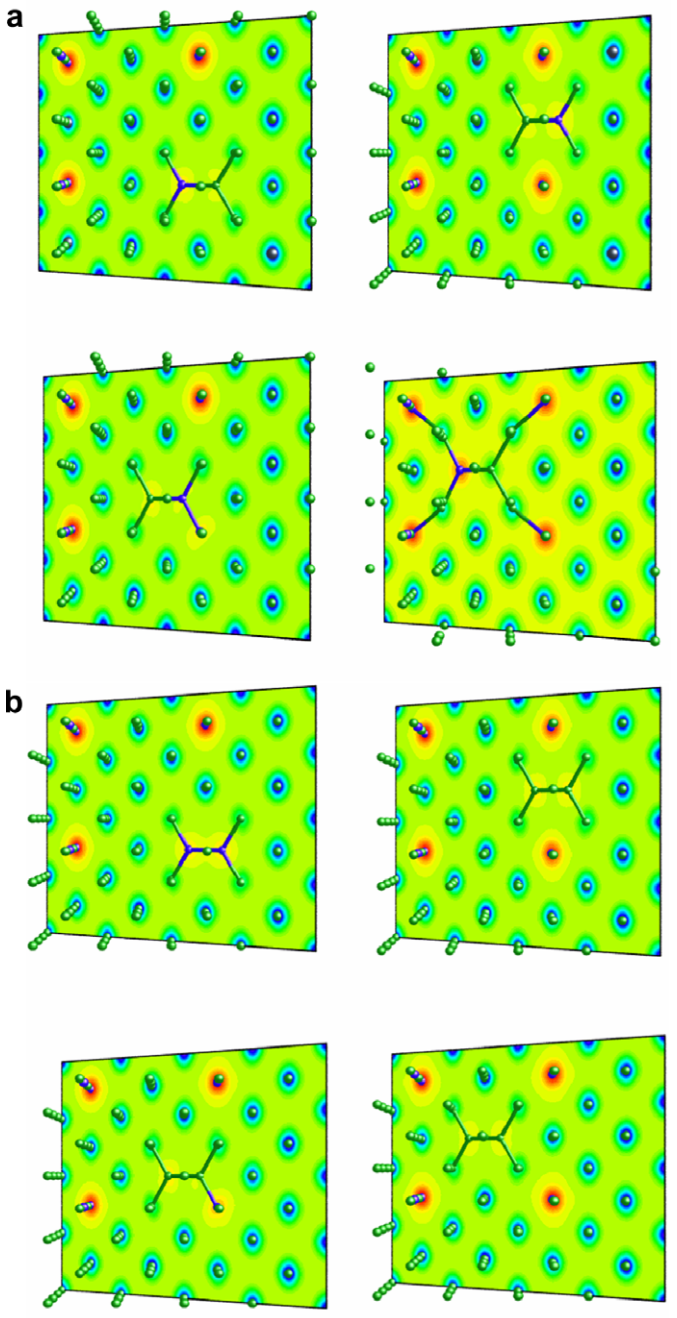

Fig. 3. Spin density maps projected on (1 1 0) plane and calculated for (a) mixed Fe–Cr dumbbells and (b) Fe–Fe and Cr–Cr ⟨1 1 0⟩ dumbbells at various positions within the ordered phase $Fe_{15}Cr$. Clockwise from the top right are the configurations at site Fe1, Fe_3, Fe and Cr, respectively.

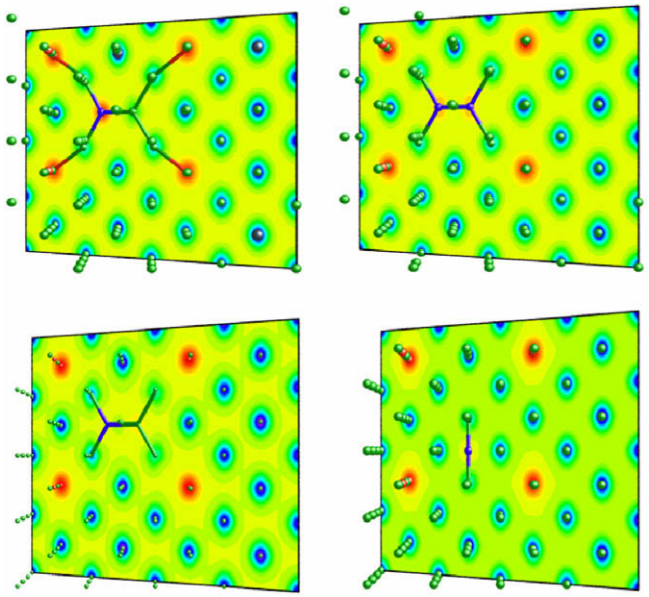

Fig. 4. Clockwise from the top right: spin density maps calculated for ⟨1 1 0⟩ Mn–Mn, C in octahedral, Fe–C and Fe–Mn mixed dumbbells at Fe_3 site.

5. Environmentally magnetic dependence of vacancy migration barrier

One of very challenging problems for modelling the precipitation kinetics in concentrated alloys at a microscopic scale is the dependence of saddle point energies of defect migration on the local atomic configurations. For ferritic/martensitic steels in general and for the Fe–Cr binary system in particular, this environmental

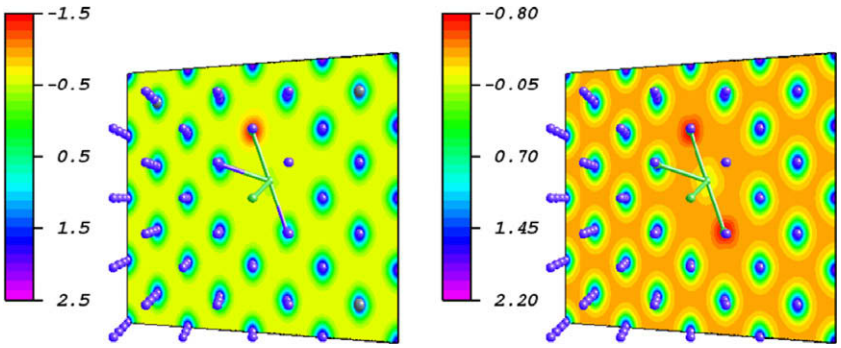

Fig. 5. Spin density maps calculated for saddle point configuration of exchange vacancy-Cr migration within different environments: with 6Fe atoms (right) and with 3Cr + 3Fe atoms (left).

dependence is again correlated with magnetic moment distribution in these configurations. In the bcc lattice, there are six nearest neighbours of the saddle point position for a point defect [20]. Fig. 5 shows the spin density maps calculated for two saddle point energy configurations obtained by nudge elastic band method implemented in the VASP code for the jumping Cr atom and mono-vacancy in bcc-Fe. The left hand side configuration containing 3Cr and 3Fe atoms among the nearest neighbours has the highest vacancy migration barrier of 0.89 eV whereas the right hand side one with 6Cr atoms in its environment has the lowest saddle point binding energy of 0.56 eV [2]. For the first configuration, the calculated magnetic moments on 3Cr atoms are $-1.27\mu_B$ whereas for the latter one, the magnetic moments on 6Cr atoms are decreased to $-0.76\mu_B$. The different magnetic behaviour of these two configurations can be seen clearly in Fig. 5 that shows the scale of magnetic moments. We find that lower anti-ferromagnetic moment configuration of environmental Cr atoms corresponds to smaller migration barrier for an exchange between vacancy and chromium. Note that in the solid solution limit the migration barriers of the Fe atoms are usually higher than those of Cr atoms [2].

6. Summary

We have demonstrated in this paper that the anomalous thermodynamic and defect properties in concentrated Fe–Cr binary alloys are strongly correlated with magnetic properties obtained from the first-principle spin density map calculations. We have illustrated this correction for the case of ordered $Fe_{15}Cr$ phase where there is a consistent result of negative enthalpy of mixing between various investigations: DFT, cluster expansion in combination with exchange Monte Carlo and the present TBSM approach. We show that the mixed dumbbell $\langle 1\,1\,0\rangle$ Fe–Cr has a positive binding energy and its origin can be explained by anti-ferromagnetic alignment of Cr at the SIA configuration. Furthermore, the same behaviour is also found for the mixed dumbbell Fe–Mn where the strain field argument from classical elastic theory fails, whereas in the case of Fe–C impurity interaction the size effect is dominant because of negligible magnetic effect on the carbon atoms. Finally, it is shown that the magnetic interaction plays an important role in understanding the environmental dependence of vacancy-Cr exchange migration barrier that is crucial for investigating the precipitation kinetics in Fe–Cr alloys.

Acknowledgements

The work, supported by the UK Engineering and Physical Sciences Research Council and European Communities under the contact of association between EUROATOM and UKAEA, was carried out within the framework of the European Fusion Development Agreement (Task No. D051-TW6-TTMS-007). The views and opinions expressed herein do not necessary reflect those of European Commission.

References

[1] E.A. Little, Mater. Sci. Technol. 22 (2006) 491.
[2] D. Nguyen-Manh, M.Yu. Lavrentiev, S.L. Dudarev, C.R. Phys. 40 (2008) 379.
[3] M.Yu. Lavrentiev, R. Drautz, D. Nguyen-Manh, P.T.C. Klaver, S.L. Dudarev, Phys. Rev. B. 75 (2007) 014208.
[4] M. Hennion, J. Phys. F: Met. Phys. 13 (1983) 2351.
[5] P. Olsson, I.A. Abrikosov, I. Vitos, J. Wallenius, J. Nucl. Mater. 321 (2003) 84.
[6] A.A. Mirzoev, M.M. Yalalov, D.A. Mirzaev, Phys. Met. Metall. 97 (2004) 4336.
[7] S.L. Dudarev, P.M. Derlet, in: P. Gumbsch (Ed.), Proceedings of the Third International Conference on Multiscale Materials Modelling, Freiburg, Germany, 18–22 September 2006, Fraunhofer Institute for Mechanics of Materials, 2006, pp. 713–720.
[8] G. Kresse, J. Hafner, Phys. Rev. B 47 (1993) R558;
G. Kresse, J. Hafner, Phys. Rev. B 49 (1994) 14251.
[9] G. Kresse, J. Furthmuller, Comput. Mater. Sci. 6 (1996) 15.
[10] G.Q. Liu, D. Nguyen-Manh, B.G. Liu, D.G. Pettifor, Phys. Rev. B 71 (2005) 174115.
[11] D. Nguyen-Manh, A.P. Horsfield, V. Vitek, Prog. Mater. Sci. 52 (2007) 255.
[12] I. Yang, S.Yu. Savrasov, G. Kotliar, Phys. Rev. Lett. 87 (2003) 216405.
[13] P.T.C. Klaver, R. Drautz, M.W. Finnis, Phys. Rev. B 74 (2006) 224207.
[14] A.L. Nikolaev, J. Phys.: Condens. Matter 11 (1999) 8633.
[15] D. Nguyen-Manh, M.Yu. Lavrentiev, S.L. Dudarev, in: P. Gumbsch (Ed.), Multiscale Materials Modelling, Freiburg, Germany, 2006, p. 767;
D. Nguyen-Manh, M.Yu. Lavrentiev, S.L. Dudarev, J. Comput. Mater. Design (2008).
[16] C.C. Fu, F. Willaime, P. Ordejon, Phys. Rev. Lett. 92 (2004) 175503.
[17] D. Nguyen-Manh, A.P. Horsfield, S.L. Dudarev, Phys. Rev. B 73 (2006) 020101R.
[18] P.M. Derlet, D. Nguyen-Manh, S.L. Dudarev, Phys. Rev. B 76 (2007) 054107.
[19] R.G. Faulkner, S.H. Song, P.E.J. Flewitt, Mater. Sci. Technol. 12 (1996) 904.
[20] Y. Le Bouar, F. Soisson, Phys. Rev. B 65 (2002) 094103.